Research Square

Preprints are preliminary reports that have not undergone peer review.
They should not be considered conclusive, used to inform clinical practice,
or referenced by the media as validated information.

Blood-brain barrier disruption in Long COVID-associated cognitive impairment

Matthew Campbell (matthew.campbell@tcd.ie)
Trinity College Dublin https://orcid.org/0000-0003-3325-240X
Chris Greene
Trinity College Dublin https://orcid.org/0000-0003-4192-9433
Ruairi Connolly
Trinity College Dublin
Declan Brennan
Trinity College Dublin
Aoife Laffan
St James' Hospital
Eoin O'Keeffe
Trinity College Dublin
Lilia Zaporojan
St James' Hospital
Emma Connolly
Trinity College Dublin
Cliona Ni Cheallaigh
Trinity College, Dublin
Niall Conlon
St James' Hospital
Colin Doherty
Trinity College Dublin

Article

Keywords: SARS-CoV-2, long COVID, blood-brain barrier, brain fog

Posted Date: September 22nd, 2022

DOI: https://doi.org/10.21203/rs.3.rs-2069710/v1

License: This work is licensed under a Creative Commons Attribution 4.0 International License.
Read Full License

Abstract

Vascular disruption has been heavily implicated in COVID-19 pathogenesis and may predispose the neurological sequelae associated with the condition now known as long COVID. To date, no studies have objectively assessed blood-brain barrier (BBB) function in individuals with neurological complications stemming from prior SARS-CoV-2 infection. Here, we explored the neurobiological effects of SARS-CoV-2 infection in humans with acute infection (n = 76) and those with persistent long COVID with and without neurological impairment. Following acute infection, patients with neurological impairment had increased serum S100β, indicative of BBB disruption. Furthermore, using dynamic contrast-enhanced magnetic resonance imaging (DCE-MRI) in long COVID patients (n = 32), we observed elevated BBB permeability in distinct neuroanatomical regions including the frontal cortex, occipital lobe and temporal lobes which correlated with global brain volume and white matter volume deficits in patients with neurological impairment. Patients with neurological impairment had increased levels of blood-based biomarkers including GFAP, TGFβ and IL8 with levels of TGFβ that correlated with BBB permeability and structural brain changes. Peripheral blood mononuclear cells isolated from unaffected and long COVID patients had persistent upregulation of inflammatory markers including IFNA/G and showed increased adhesion to human brain endothelial cells *in vitro*. Finally, exposure of endothelial cells to serum from long COVID patients induced increases in ICAM-1, VCAM-1 and TNF irrespective of neurological sequelae. Together, these data suggest that sustained systemic inflammation and persistent localised BBB dysfunction is a feature of long COVID-associated neurological impairment. Importantly, this may also be therapeutically relevant in the treatment and clinical management of this patient group.

Introduction

Coronavirus disease 2019 (COVID-19) is a clinical syndrome caused by a novel coronavirus, severe acute respiratory syndrome coronavirus-2 (SARS-CoV-2). COVID-19 primarily affects the respiratory tract and can progress to respiratory compromise, severe acute respiratory distress syndrome and death[1,2]. Neurological sequelae of COVID-19, colloquially known as “brain fog” are increasingly being reported and include headache, fatigue, malaise and altered levels of consciousness. Acute respiratory distress syndrome (ARDS) due to COVID-19 has been associated with encephalopathy, agitation, confusion, and corticospinal tract dysfunction. Such symptoms however, including anosmia (although not to the extent seen in the first wave of COVID-19), may be expected in anyone recovering from a severe viral illness due to cytokine release, critical illness encephalopathy, or medication[3]. Clinical observations of neurological complications in 236,379 patients in the 6 months following a COVID-19 diagnosis have found that 33.62% of patients were estimated to have demonstrated clinically significant neurological or psychiatric dysfunction[4]. Neurological problems have been reported in other respiratory viral infections including influenza, coronavirus and metapneumovirus with febrile or afebrile seizures, status epilepticus, encephalopathies and encephalitis being the most frequently reported[5]. However, there is still little understanding of the pathogenesis and long-term outcome of neurological problems following SARS-CoV-2 infection. SARS-CoV-2 gains cellular entry via its receptors ACE2 and TMPRSS2, but it may enter

via other receptors including neuropilin and vimentin, all of which are enriched in vascular cells[6–10]. There are, however, conflicting reports regarding the neuro-invasiveness of SARS-CoV-2 and indeed the cellular expression of the receptors[11–15], suggesting that other mechanisms are responsible for the neurological problems reported. A recent preprint suggests persistence of viral RNA in multiple anatomic sites including the brain for up to 230 days following symptom onset, though, these data are from post-mortem donor tissues which represent the sickest of individuals[16].

One hypothesis suggests that breakdown to the integrity of the blood-brain barrier (BBB) and subsequent brain penetration of serum components is responsible for the neurological manifestations following SARS-CoV-2 infection. The BBB is formed by endothelial cells lining cerebral blood vessels and supported by surrounding cells including astrocytes, pericytes, microglia, neurons and the acellular basement membrane[17]. The barrier is characterised by an enrichment of interendothelial tight junction proteins, a variety of luminal and abluminal transporters and luminal efflux transporters which together maintain separation of the blood and brain and tightly regulate molecular trafficking between the blood and brain and vice versa[18].

There is clear evidence of microvascular injury in the brains of deceased COVID-19 patients, including fibrinogen leakage, and thinning of the endothelial cell basal laminae in the olfactory bulb[13,19]. A more comprehensive evaluation of the same cohort using spatial transcriptomics revealed more detailed vascular and immunological features of microvessels in the brain including serum protein extravasation, platelet accumulation and coagulation system activation[20]. Numerous studies have also examined BBB-related changes and responses to SARS-CoV-2 infection or spike protein treatment in post-mortem tissue and animal models[13,14,19,21–35]. Indeed, it has been shown that the spike protein can cross the BBB in rodents which may cause neuroinflammation and cognitive changes[32]. However, the cerebrovascular pathology in patients and the underlying mechanisms are still unclear, especially in individuals with long COVID.

The lack of a specific neurological signature of the disease is interesting as other zoonotic beta-coronaviruses often produce robust and predictable neurological injury[36]. In humans, data from SARS and MERS also shows that neurological injury in humans is rare, strongly suggesting that, normally, the BBB provides robust neuroprotection from viral CNS invasion in the majority of patients[37]. The clinical manifestation of SARS-CoV2 induced BBB alterations in patients have not yet been reported.

Here, we hypothesised that the neurological response to COVID may be due to BBB breakdown and subsequent extravasation of serum components. We show that BBB disruption is evident in acute neurological COVID patients and that a cohort of patients with persistent “brain fog” have BBB disruption on neuroimaging which was associated with circulating biomarkers of neuroinflammation and BBB breakdown. We suggest that measurement of BBB integrity may be a clinically useful biomarker of the neurological sequelae that is associated with COVID-19 in some patients. Added to this, targeted

regulation of BBB integrity may also represent a novel method of clinically managing patients with long COVID.

Results

Acute COVID-induced brain fog is associated with BBB dysfunction

We obtained serum samples from 76 in-patients with acute COVID-19 recruited as part of the St James Hospital STTAR Bioresources collection during the initial wave of COVID-19 in March/April 2020 (Fig. 1a)[38]. 25 unaffected control samples were collected prior to the COVID-19 pandemic. The mean age of control and COVID samples was 44 and 44.7 respectively. The most frequent presenting symptoms included dyspnoea (47), loss of smell and taste (46), cough (45), fatigue (40) and fever (36). As previously reported, more males than females had severe COVID (***$p < 0.001$) and more males required supplemental oxygen (**$p = 0.002$) (Table 1). Serum samples were screened on a Luminex 10-plex kit for inflammatory and BBB dysfunction markers. Severity of COVID-19 was determined according to the WHO Severity Guidelines with 25 unaffected, 43 mild, 10 moderate and 23 severe. We found a significant increase of IL8 (**$p = 0.01$ vs unaffected) in moderate cases. There was a significant increase in TNF (**$p = 0.004$ vs unaffected; **$p < 0.002$ vs mild), IL6 (**$p = 0.002$ vs unaffected; ***$p < 0.001$ vs mild) and IL8 (***$p < 0.001$ vs unaffected; *$p = 0.03$ vs mild) cytokines in severe COVID-19 patients (Fig. 1a). Stratification of patients according to presence or absence of brain fog revealed a significant increase in serum concentrations of TNF (**$p = 0.003$), IL6 (***$p < 0.001$), IL8 (**$p = 0.008$) and S100β (*$p = 0.010$) in brain fog patients after controlling for age, sex and severity of infection (Fig. 1c). There was a significant increase in serum concentrations of TNF (***$p < 0.001$), IL6 (***$p < 0.001$) and IL8 (*$p = 0.038$) in patients requiring supplemental oxygen (Figure S1a) while there was a significant increase in TNF (**$p = 0.005$), IL6 (***$p < 0.001$) and IL8 (*$p = 0.046$) in patients requiring hospitalisation (Figure S1b). Spearman's partial correlation analysis revealed a significant correlation between WHO Severity of COVID-19 and serum concentrations of TNF, IL6 and IL8 ($r = 0.367$, ***$p = 0.002$; $r = 0.425$, ***$p < 0.001$; and $r = 0.231$, *$p = 0.047$ respectively after adjusting for age and sex) (Figure S2a-c). Of the 76 patients, 36 had a second blood sample drawn owing to deterioration of clinical symptoms so serum concentrations of all analytes were assessed between timepoint 1 and 2 (T1 and T2) to monitor disease progression. There was a significant increase in serum concentrations of IL8 (***$p < 0.001$ Wilcoxon signed-rank test) between T1 and T2 (Figure S3).

BBB dysfunction is associated with Long COVID-induced cognitive impairment

Given the significantly increased serum concentrations of S100β our data indicated that active/acute SARS-CoV-2 infection is associated with BBB dysfunction in individuals with neurological impairment. To directly visualise BBB function, we recruited 10 recovered and 22 Long COVID patients who were diagnosed with COVID-19 during the first outbreak of disease in Ireland in April 2020 (Figure 2a and Table

2). All participants were recruited from St James Hospital Dublin and were PCR confirmed cases of COVID-19. None of the patients in this cohort had received a vaccine. We used a quick smell identification test (Q-SIT) based method to determine objective anosmia status in participants and determined a strong correlation of reported anosmia status and Q-SIT score, providing an excellent readout of the utility of objective anosmia measurement in prolonged anosmia after COVID-19. Participants were grouped according to the presence or absence of brain fog (brain fog (-) or brain fog (+)). We hypothesised that COVID-19 associated cognitive impairment may be a strong predictor of BBB disruption in COVID-19 patients. Brain fog patients reported a mean symptom duration of 222.75 days while non-brain fog participants had a mean symptom duration of 170.55 days. Participants were scanned an average of 146 days following SARS-CoV-2 infection (Table 2). 16 (50 %) participants reported anosmia which was confirmed by Q-SIT testing (average score 1/3; 159 +/- 88 days duration) at the time of scanning. 6 participants (all brain fog) showed mild-moderate cognitive impairment on the MOCA test (score 18-25) along with deficits in recall, executive function and word finding (Table 2).

While standard diagnostic MRI scans showed no pathological findings in any participant, DCE-MRI imaging revealed significantly increased whole brain leakage in COVID-19 patients with brain fog (Figure 2b-d) with increased percentage of brain volume with leaky blood vessels in the brain fog cohort compared to the cohort without brain fog (***p<0.001). Stratifying the cohort into recovered, long COVID without brain fog and long COVID with brain fog revealed significantly increased BBB permeability in the brain fog cohort compared to recovered (*p=0.014) and long COVID without brain fog (***p<0.001). Region of interest analysis identified significantly increased leakage in the right and left temporal lobes (p***<0.001 and p=0.005 respectively) and right and left frontal cortex (**p=0.005 and **p=0.004 respectively) (Figure 2e-i). Stratifying the groups according to recovered, long COVID or brain fog revealed significantly increased BBB permeability in the brain fog group only in the right (**p=0.007 vs recovered; **p=0.008 vs long COVID) and left (*p=0.035 vs recovered; p=0.051 vs long COVID) temporal lobe and right (*p=0.015 vs long COVID) and left (*p=0.05 vs recovered; *p=0.025 vs long COVID) frontal cortex (Figure S4a-e). There was no association between BBB permeability and anosmia status, duration of anosmia, Q-SIT or MOCA scores (Figure S5), however regional BBB permeability in the right (r=0.546, **p=0.002) and left (r=0.532, **p=0.002) temporal lobes correlated with the duration of anosmia.

Long COVID associated brain fog induces structural changes in the brain

To explore if there were structural brain changes accompanying increased BBB permeability in our cohorts, we conducted volume and thickness measurements on recovered, long COVID and 60 age-matched healthy controls from the publicly available IXI dataset (Table 2) and examined global brain volume, cerebrospinal fluid (CSF) volume and right and left volumes of cerebral and cerebellar white and grey matter and brainstem, hippocampus, and amygdala. Comparing individuals with prior COVID infection to unaffected revealed volumetric deficits predominantly in the frontal and temporal lobes and increases in the lateral ventricles and occipital lobes (Figure 3a) while groupwise comparisons of macrostructures revealed decreased global brain volume in brain fog patients (**p=0.001) along with significantly reduced cerebral white matter volume in both hemispheres in the recovered (***p<0.001) and

brain fog (***p<0.001) cohorts along with reduced cerebellar white matter volume in recovered (***p<0.001, right; **p=0.006, left), long COVID (**p=0.01, right; *p=0.049, left) and brain fog (***p<0.001, right and left) cohorts (Figure 3b-e and Table 3). There was significantly increased CSF volume in the brain fog cohort only (**p=0.005) (Figure 3f and Table 3). Cortical thinning was also evident predominantly in the temporal and frontal lobes when looking at all patients with prior SARS-CoV-2 infection compared to unaffected controls (Figure 3g). When comparing groups, there was reduced thickness in the fontal pole in recovered (**p=003), long COVID (**p=0.002) and brain fog (***p<0.001); superior frontal gyrus in long COVID (**p=0.003) and brain fog (**p=0.002); middle temporal gyrus in brain fog only (*p=0.016); and superior temporal gyrus (***p<0.001) in brain fog only. Spearman partial correlations revealed significant negative associations between the number of BBB disrupted voxels with global brain volume (r=-0.528, **p=0.002), right (r=-0.424, *p=0.022) and left (r=-0.466, *p=0.011) white matter volume, and right (r=-0.503, **p=0.005) and left (r=-0.493, **p=0.007) cerebral volume and was positively associated with CSF volume (r=0.532, **p=0.002) (Figure 4a-g).

Immunovascular dysregulation in long COVID blood samples

Finally, we analysed blood-based biomarkers of neuroinflammation and BBB dysfunction in the long COVID cohort. We selected markers previously associated with BBB dysfunction, neuroinflammation and chronic fatigue syndrome including S100β, GFAP, TGFβ, IL6, IL8 and CCL2. Individuals with brain fog had significantly increased GFAP (*p=0.022), TGFβ (**p=0.004) and IL8 (*p=0.0427) compared to unaffected, recovered, and long COVID without brain fog. Levels of phosphorylated TAU, sICAM1 and S100β were comparable between groups (Figure 5a-e). This differs from the blood analysis of the patients with acute COVID and suggests a temporal change in the utility of these markers for prognosis and clinical management. Next, we performed Spearman partial correlation analysis adjusting for age and sex to identify any associations between neuroinflammatory/BBB dysfunction markers with BBB permeability assessed by DCE-MRI. Levels of TGFβ were significantly associated with the percentage of brain volume displaying leaky blood vessels (r=0.501, **p=0.008) as well as with global brain volume (r=-0.394, *p=0.042), CSF volume (r=0.438, *p=0.020), brainstem volume (r=-0.656, p<0.001) and amygdala volume (r=-0.402, *p=0.038) (Figure 5f-j and Figure S6).

White blood cells from COVID patients activate brain endothelial cells

Given the prevalence of circulating markers indicative of BBB dysfunction and immune cell activation, we examined gene expression changes in PBMCs isolated from long COVID patients which revealed increased expression of interferon signalling components and inflammatory markers independent of neurological impairment indicating sustained inflammatory responses in all groups including recovered individuals (Figure 6a-f). We next examined immunovascular interactions in PBMCs isolated from patients with COVID and found increased adhesion of PBMCs to human brain endothelial cells in the long COVID group compared to unaffected (***p<0.001) which was heightened in the presence of TNF (**p=0.0031 vs control) (Figure 6g, h). Furthermore, exposure of human brain endothelial cells to 10% serum from recovered, and long COVID groups resulted in the upregulation of *ICAM1* (**p=0.0081),

VCAM1 (*p=0.0127) and *TNF* (**p=0.004) transcripts compared to unaffected sera (Figure 6i-l). Exposure of human brain endothelial cells to S1 spike protein had similar effects with dose-dependent increases in *TNF* (*p=0.045), *TGFβ* (*p=0.017), *ICAM1* (p=0.057) and *VCAM1* (***p<0.001) (Figure S7) following 72 hours treatment with 0-400 nM S1 spike protein.

Discussion

Overall, our results suggest that long COVID “brain fog” is associated with impairment of BBB function and increased expression of systemic inflammatory and BBB dysfunction markers including GFAP, TGFβ and IL8. BBB dysfunction was unique to the brain fog cohort in our study with sustained dysfunction up to one year following recovery from active infection with dysfunction evident in multiple neuroanatomical regions including the temporal lobes and frontal cortex. We found no evidence of BBB dysfunction in patients with anosmia without accompanying brain fog suggesting that cerebrovascular dysfunction in the olfactory bulb does not clearly drive this condition. It has been shown instead that accumulation of infiltrating T-cells expressing interferon-gamma results in reduction of olfactory sensory neurons relative to support cells in patients with long COVID associated anosmia[39]. It is possible that this sustained inflammatory response in the olfactory epithelium results in cerebrovascular damage in the olfactory bulbs and higher resolution MRI could help to tease out these changes. We did observe a significant correlation between BBB disruption in the temporal lobes with the duration of anosmia. The temporal lobe contains important regions that form part of the primary olfactory cortex including the piriform cortex, amygdala and entorhinal cortex with direct connections from and to the olfactory bulb encompassing regions of the piriform cortex, parahippocampal gyrus and entorhinal cortex along with orbitofrontal areas[40–42]. The hippocampus is also important for odour recognition memory and it is possible that BBB dysfunction in these regions contributes to anosmia or hyposmia[41]. In the brain fog cohort, we found evidence of reduced global brain volume along with reductions in white matter in cortical and cerebellar tissue that was also apparent in individuals who had recovered from infection suggesting that these changes do not drive the fatigue and cognitive slowing associated with brain fog in this condition. Other groups have also found changes on neuroimaging following mild infection. Initial systemic neuropathological changes in patients with COVID-19 appeared to be mild, with marked brainstem neuroinflammation the most common finding[43]. In a three-month follow up MRI study of COVID-19 patients, higher grey matter volumes were found in several cerebral territories, including the olfactory cortices, hippocampi, and cingulate gyri which may be a marker of acute or sub-acute inflammation[43]. A recent large cohort study revealed longitudinal changes in brain volume and cortical thinning following mild SARS-CoV-2 infection[42]. Neuroimaging has also been used to detect other cerebrovascular changes in the brain following SARS-CoV-2 infection. Abnormalities detected include cerebral microbleeds, hypometabolism and cerebral hypoperfusion in several brain regions[29,44–47].

BBB dysfunction was evident in individuals suffering acute neurological impairment during the active phase of SARS-CoV-2 infection with increased serum levels of the astrocytic protein S100β together with increased expression of TNF and IL6 after adjusting for age, sex, and severity of infection. This suggests that a heightened inflammatory response in this neurological cohort may drive BBB dysfunction. Serum

levels of S100β have previously been found elevated in several neurological disorders including epilepsy, traumatic brain injury and schizophrenia[48–50]. However, longitudinal studies will be required to determine if BBB disrupted acute COVID patients are more likely to develop long COVID-associated brain fog.

We also found increased expression of IL8 in individuals with deteriorating clinical symptoms. In the long COVID cohort, levels of IL8, GFAP and TGFβ were elevated in the brain fog group only. GFAP is a marker of cerebrovascular damage and has previously been shown to be elevated following repetitive head trauma, reflecting BBB disruption, as seen in contact sport athletes[24,51]. Interestingly, TGFβ was strongly associated with the number of BBB disrupted blood vessels along with global brain volume and white matter volume changes. TGFβ has been implicated in the pathogenesis of chronic fatigue syndrome, a condition noted for its overlap of brain fog with COVID[52–54].

Several studies have examined BBB function in animal models of SARS-CoV-2 infection and in post-mortem tissue to understand the impact of acute infection on BBB integrity. The spike protein of SARS-CoV-2 was shown to cross the BBB while direct intrahippocampal injection induced cognitive deficits and anxiety-like behaviour in mice[32,55]. In samples from patients who died during the initial wave of COVID in 2020, Lee *et al.* showed fibrinogen extravasation and evidence of overactivation of the coagulation system[19,20] while Wenzel *et al.* found string vessels, pathological blood vessels without endothelial cells[25]. A few studies have also examined changes in systemic markers in convalescent COVID patients and pinpoint to strong upregulation of biomarkers of inflammation and innate immunity and downregulation of platelet-related pathways[56]. Persistent immune activation has also been reported in individuals with long COVID up to 8 months post infection[57].

Long COVID is a significant burden in many patients post recovery from COVID-19. Patients describe fatigue, memory loss, dyspnoea as some of the key symptoms of long COVID, while another subset of patients describe “brain fog” like that commonly reported in post-concussive syndrome and chronic fatigue syndrome[58,59]. In this study, we assessed BBB integrity in a series of patients who had recovered from infection but had symptoms persisting up to 1 year following infection. Our data suggest that BBB disruption is strongly associated with long COVID-associated cognitive impairment with regional differences in BBB integrity in long COVID patients displaying brain fog. Our biomarker analysis in acute COVID patients suggests that a subset of infected individuals with acute cognitive impairment have a disrupted BBB as determined by serum presence of the astrocytic protein S100β. This study is the first to focus on long COVID patients with or without neurological impairment and compare them to individuals who recovered from a previous SARS-CoV-2 infection. Individuals with brain fog have persistent BBB dysfunction which could be detected by DCE-MRI and plasma assessment of circulating biomarkers. This provides the first objective evidence for a link between BBB disruption and cognitive impairment within a cohort of patients with long COVID. Further longitudinal studies will be required to examine changes in BBB permeability over time, however, targeted regulation of BBB integrity could now potentially be considered for the treatment of patients with brain fog associated with long COVID.

Methods

Study participants

Participants included recovered COVID-19 patients, male or female aged 18 and above with and without neurological symptoms. Participants with long COVID, with symptom persistence over 12 weeks from infection were also recruited. Candidates were excluded if they had a history of a neurological disorder that may better explain the results of the study such as epilepsy, brain trauma, neuropsychiatric disorder, or mild cognitive impairment. Suitable candidates proceeded to assessment with DCE-MRI imaging, Q-SIT olfactory testing and a review of pulmonary imaging and haematological parameters at the time of COVID-19 diagnosis. The Joint Research Ethics Committee (JREC) of St James's and Tallaght Hospital's approved the study and informed consent was obtained from all participants. Research was performed according to the principles of the Declaration of Helsinki. The legal basis for the Study was consent according to GDPR principles.

Olfactory Testing

Participants olfactory function was assessed using the quick smell identification test (Q-SIT). The Q-SIT is a standardised and validated three item odour identification screen[60]. A score of 2 or more is a normal test and cut-off score of 1 or less is an abnormal test for anosmia. Q-SIT has displayed high positive and negative predictive value in detecting olfactory dysfunction in COVID-19 patients. In addition, the Q-SIT is a tear-off card test is disposable so there is no concern about contamination and transmission of disease form COVID-19 patients[61].

Dynamic contrast-enhanced magnetic resonance imaging

BBB permeability maps were created using the slope of contrast agent concentration in each voxel over time, calculated by a linear fit model as previously described[62,63]. Thresholds of high permeability was defined by the 95th percentile of all slopes in a previously examined control group. Imaging was performed with a 3T Philips Achieva scanner. Sequences included a T1- weighted anatomical scan (3D gradient echo, TE/TR =3/6.7 ms, acquisition matrix 268x266, voxel size: 0.83x0.83x.9mm), T2-weighted imaging (TE/TR =80/3000 ms, voxel size: 0.45x0.45x.4mm), FLAIR (TE/TR =125/11000 ms, voxel size:0.45x0.45x4mm). For the calculation of pre-contrast longitudinal relaxation time (T10), the variable flip angle (VFA) method was used (3D T1w-FFE, TE/TR = 2.78/5.67 ms, acquisition matrix: 240x184, voxel size: 0.68x0.68x5 mm, flip angles: 2, 10, 16 and 24°). Dynamic contrast enhanced (DCE) sequence was then acquired (Axial, 3D T1w-FFE, TE/TR = 2.78/5.6 ms, acquisition matrix: 240x184, voxel size: 0.68x0.68x5 mm, flip angle: 6°, Tt = 6.5 Sec, temporal repetitions: 61, total scan length: 22.6 minutes). An intravenous bolus injection of the contrast agent gadobenate dimeglumine (Gd-BOPTA, Bracco Diagnostics Inc., Milan, Italy) was administered using an automatic injector after the first three DCE repetitions. To control for interindividual variabilities due to heart rate, blood flow or rate of contrast injection, each voxel's leakage rate was normalised to that of the superior sagittal sinus. The percent of suprathreshold voxels was used as a measure reflecting global BBB leakage.

Volumetric and thickness measurements

T1-weighted anatomical images were uploaded to the VolBrain online brain volumetry software (https://volbrain.upv.es)[64], and analysed with vol2brain 1.0 which is an online pipeline that registers images to the Montreal Neurological Institute (MNI) space, and reports the volumes of expert-labelled anatomical structures as percentage of total intracranial volume. We analysed the volume of the right/left cerebral and cerebellar grey/white matter, frontal, temporal, parietal and occipital and CSF along with thickness of the frontal, parietal, occipital and temporal lobes. All volume data was normalised to total intracranial volume (TIV) which is the sum of grey matter, white matter and CSF. Volumes were expressed as a percentage of TIV. 60 age and sex matched healthy control scans were randomly selected from the IXI dataset (https://brain-development.org/ixi-dataset/) which represents 10 % of the entire dataset. All scans were performed on the same Philips 3T system at Hammersmith Hospital. Volumetric maps for comparisons between COVID positive and negative groups were generated in xjview following automatic brain segmentation in the CAT12 toolbox with default parameters and subsequent smoothing with an 8 mm kernel. Thickness maps for comparisons between COVID positive and negative groups were generated in CAT12 toolbox run in SPM12 in MATLAB R2021a following brain segmentation as above and smoothing with a 15 mm kernel. Two-sample t-test was used for statistical analysis with age, sex and TIV as covariates.

Sample collection

Blood samples were collected into serum separator tubes and EDTA-coated tubes for serum and PBMC isolation respectively. Serum was separated by centrifugation at 2000 rpm for 10 min at room temperature. PBMCs were separated via layering of blood samples diluted twofold in PBS (ThermoFisher, #14190) over Lymphoprep^{TM} density gradient medium (Stemcell Technologies, #07851) followed by centrifugation at 400 rcf for 25 min at room temperature at 0 break and 0 acceleration. Plasma was collected and PBMC layer was collected into a new 50 ml falcon tube, resuspended to 50 ml with PBS and centrifuged at 2000 rpm for 5 min at room temperature. PBMCs were resuspended in 50 ml PBS and centrifuged at 1000 rpm for 10 min at room temperature. PBMCs were resuspended to 2 x 10^6 cells/ml in RPMI 1640 media with L-glutamine (Lonza, #LZBE12-702F) supplemented with 50 % fetal bovine serum (Merck, #F7524) and 10 % DMSO (Merck, #D5879) and frozen at -80^{0}C overnight before being moved to liquid nitrogen.

Luminex assay

A 10-plex Luminex assay (R&D Systems, #LXSAHM-10) was used for cytokine profiling. Serum samples were diluted twofold in sample dilution buffer. Then, 50 µl of sample or standard were pipetted in duplicate into each wall of an assay 96 well plate. 50 µl of diluted Microparticle Cocktail were added to each well, the plate was covered and incubated for 2 hours at room temperature on a shaker at 300 rpm. Wells were washed 3 times with Wash Buffer before addition of 50 µl of diluted Biotin-Antibody Cocktail. The plate was covered and incubated for 1 hour at room temperature on a shaker at 300 rpm. Wells were

washed as above before addition of 50 µl of diluted Streptavidin-PE to each well. The plate was covered and incubated for 30 min at room temperature on a shaker at 300 rpm. Wells were washed as above before microparticles were resuspended in 100 µl of Wash Buffer. The plate was incubated for 2 min at room temperature on a shaker at 300 rpm and was read on a MAGPIX plate reader (Luminex).

Dot blot

Plasma samples were spotted (2 µl) onto 0.2 µm nitrocellulose membrane (Whatman, #10401391) and allowed to dry for 30 minutes. Membranes were blocked in 5 % bovine serum albumin (BSA, Merck, #A7906) in phosphate buffered saline supplemented with 0.1 % Triton X-100 (PBST) for 1 hour at room temperature. Membranes were incubated overnight in primary antibody in blocking buffer. Membranes were washed three times for five minutes each in PBST, followed by incubation in secondary HRP-conjugated antibodies. Membranes were washed three times for five minutes each in PBST and incubated with strong ECL substrate (Advansta, #K-12045-D50) for 2 min before being developed on a C-Digit (LiCor). Protein bands were quantified in ImageJ (National Institutes of Health, Rockville, MD, USA). Primary antibodies used were mouse anti-GFAP (1/500, Merck, #G3893), rabbit anti-TGFβ (1/500, Abcam, #ab92486) and mouse anti-Phospho-Tau (1/500, Fisher Scientific, #10599853). Secondary antibodies used were anti-mouse HRP (1/5000, Merck, #A4416) and anti-rabbit HRP (1/5000, Merck, #A6154).

RT-qPCR

RNA was isolated from PBMCs and the human brain endothelial cell line hCMEC/d3 (Millipore, #SCC066) with the Omega RNA isolation kit (Omega, #R6834-02) according to manufacturer's instructions. cDNA was reverse transcribed from 500 ng RNA with the High-Capacity cDNA Reverse Transcription Kit (Applied Biosystems, # 4368814). Transcript levels were quantified on a StepOne Plus instrument (Applied Biosystems) with FastStart Universal SYBR Green Master (ROX) master mix (Roche, #04913914001). RT-PCR was performed with the following conditions: 95^0C x 2 min, (95^0C x 5s, 60^0C x 30s) x40, 95^0C x 15s, 60^0C x 1 min, 95^0C x 15s, 60^0C x 15s. Primer sequences for RT-PCR experiments are supplied in Supplementary Table 4. Relative gene expression levels were quantified using the comparative CT method (ΔΔCT). Expression levels of target genes were normalised to β-actin.

Adhesion assay

hCMEC/d3 cells were cultured in EGM2-MV growth medium (Lonza, #CC-3202) and were stimulated with 10 ng/ml recombinant human TNF-a (Peprotech, #300-01A) for 4 hours and incubated with $1x10^5$ MitoTracker Orange (ThermoFisher, # M7510) labelled PBMCs for 1 hour at 37^oC. Cells were washed three times in PBS to remove unbound PBMCs and fixed in 4 % formaldehyde (Merck, #F1635) for 10 min at room temperature. The number of adhered PBMCs was counted with the ImageJ cell counter plugin. Images were imported and converted to 8-bit and thresholded. Noise was removed with the despeckle function, and the images were converted to binary. The cell counter plugin was then used for counting adhered PBMCs. Counts were averaged from 5 images per treatment.

Serum and spike protein treatment

hCMEC/d3 cells were seeded in 12-well plates at $2x10^5$ cells/well and grown to confluence. Media was replaced with media containing 10 % serum from COVID and unaffected controls and incubated for up to 72 hours followed by RNA isolation. hCMEC/d3 cells were cultured in12-well plates as described above and stimulated with 4, 40 and 400 nM Recombinant SARS-CoV-2 Spike S1 subunit protein (R&D Systems, #BT10569) for up to 72 hours and RNA was isolated as described above.

Declarations

Ethical Approval

Informed consent was obtained from each participant. All ethical approvals were in place prior to the initiation of studies on human subjects. All experiments conformed to the principles set out in the WMA Declaration of Helsinki and the Department of Health and Human Services Belmont Report. The St James' Hospital ethics committee approved these studies.

Statistical analysis

IBM SPSS Statistics V.28 (IBM Corporation, Armonk, New York, USA) and GraphPad Prism V.9.00 (GraphPad Software, La Jolla California, USA) were used for statistical analysis. Prism 9 was used to generate charts. Categorical variables were compared between groups with x^2 tests. Normal and non-normal data were analysed with Mann-Whitney tests or ANOVA followed by Tukey or Kruskal-Wallis test respectively with age and sex adjusted p-values reported. A multivariate general linear model with age, sex and TIV as covariates was used for volumetric MRI analysis. Correlations were assessed with Pearson or Spearman rho correlation tests using partial correlations to control for age, sex and TIV. For repeated blood samples, matched samples were compared with Wilcoxon signed-rank test. To control for multiple comparisons in brain region MRI analysis and correlation analysis, false discovery rate was applied using the Benjamini-Hochberg correction. A p-value <0.05 was considered statistically significant. All quantitative PCR, ELISA and adhesion assays were performed in duplicate.

Acknowledgements

This work was supported by grants from Science Foundation Ireland (SFI), (12/YI/B2614 and 11/PI/1080), The Irish Research Council (IRC) and by a research grant from SFI under grant number 16/RC/3948 and co-funded under the European Regional Development fund by FutureNeuro industry partners. The Campbell lab is also supported by a European Research Council (ERC) grant, "Retina-Rhythm" (864522). We thank Nollaig Bourke and Matt McElheron for assistance with the Luminex assays.

Author contributions

CG: Designed research, performed experiments, collected, and analysed data, and wrote the manuscript. RC: Patient recruitment, assessment and data collection. EOK: Sample preparation. DB, AL, LZ: Patient recruitment and assessment. EC: Data maintenance and statistical analysis. CNC: Sample collection/recruitment. NC: Sample collection/recruitment. CPD: Conceived project, designed experiments and edited manuscript. MC: Conceived project, designed experiments and edited manuscript.

Competing interests

The authors declare no competing interests.

References

1. Zhu, N. *et al.* A Novel Coronavirus from Patients with Pneumonia in China, 2019. N Engl J Med **382**, 727–733 (2020). https://doi.org:10.1056/NEJMoa2001017
2. Wu, Z. & McGoogan, J. M. Characteristics of and Important Lessons From the Coronavirus Disease 2019 (COVID-19) Outbreak in China: Summary of a Report of 72 314 Cases From the Chinese Center for Disease Control and Prevention. Jama **323**, 1239–1242 (2020). https://doi.org:10.1001/jama.2020.2648
3. Helms, J. *et al.* Neurologic Features in Severe SARS-CoV-2 Infection. N Engl J Med **382**, 2268–2270 (2020). https://doi.org:10.1056/NEJMc2008597
4. *The Lancet Psychiatry* **8**, 416–427 (2021). https://doi.org:10.1016/S2215-0366(21)00084-5
5. Bohmwald, K., Gálvez, N. M. S., Ríos, M. & Kalergis, A. M. Neurologic Alterations Due to Respiratory Virus Infections. Front Cell Neurosci **12**, 386 (2018). https://doi.org:10.3389/fncel.2018.00386
6. Cantuti-Castelvetri, L. *et al.* Neuropilin-1 facilitates SARS-CoV-2 cell entry and infectivity. Science **370**, 856–860 (2020). https://doi.org:10.1126/science.abd2985
7. Amraei, R. *et al.* Extracellular vimentin is an attachment factor that facilitates SARS-CoV-2 entry into human endothelial cells. *Proceedings of the National Academy of Sciences* **119**, e2113874119 (2022). https://doi.org:10.1073/pnas.2113874119
8. Ni, W. *et al.* Role of angiotensin-converting enzyme 2 (ACE2) in COVID-19. Critical Care **24**, 422 (2020). https://doi.org:10.1186/s13054-020-03120-0
9. Hoffmann, M. *et al.* SARS-CoV-2 Cell Entry Depends on ACE2 and TMPRSS2 and Is Blocked by a Clinically Proven Protease Inhibitor. Cell **181**, 271–280.e278 (2020). https://doi.org:https://doi.org/10.1016/j.cell.2020.02.052
10. Vanlandewijck, M. *et al.* A molecular atlas of cell types and zonation in the brain vasculature. Nature **554**, 475–480 (2018). https://doi.org:10.1038/nature25739
11. Schweitzer, F. *et al.* Cerebrospinal Fluid Analysis Post-COVID-19 Is Not Suggestive of Persistent Central Nervous System Infection. Ann Neurol **91**, 150–157 (2022). https://doi.org:10.1002/ana.26262

12. Lersy, F. *et al.* Cerebrospinal Fluid Features in Patients With Coronavirus Disease 2019 and Neurological Manifestations: Correlation with Brain Magnetic Resonance Imaging Findings in 58 Patients. The Journal of Infectious Diseases **223**, 600–609 (2021). https://doi.org:10.1093/infdis/jiaa745
13. Thakur, K. T. *et al.* COVID-19 neuropathology at Columbia University Irving Medical Center/New York Presbyterian Hospital. Brain **144**, 2696–2708 (2021). https://doi.org:10.1093/brain/awab148
14. Yang, A. C. *et al.* Dysregulation of brain and choroid plexus cell types in severe COVID-19. Nature **595**, 565–571 (2021). https://doi.org:10.1038/s41586-021-03710-0
15. Iadecola, C., Anrather, J. & Kamel, H. Effects of COVID-19 on the Nervous System. Cell **183**, 16–27.e11 (2020). https://doi.org:10.1016/j.cell.2020.08.028
16. Chertow, D. *et al.* SARS-CoV-2 infection and persistence throughout the human body and brain. (2021). https://doi.org:https://doi.org/10.21203/rs.3.rs-1139035/v1
17. Abbott, N. J., Patabendige, A. A., Dolman, D. E., Yusof, S. R. & Begley, D. J. Structure and function of the blood-brain barrier. Neurobiol Dis **37**, 13–25 (2010). https://doi.org:10.1016/j.nbd.2009.07.030
18. Greene, C., Hanley, N. & Campbell, M. Claudin-5: gatekeeper of neurological function. Fluids and barriers of the CNS **16**, 3 (2019). https://doi.org:10.1186/s12987-019-0123-z
19. Lee, M.-H. *et al.* Microvascular Injury in the Brains of Patients with Covid-19. The New England journal of medicine **384**, 481–483 (2021). https://doi.org:10.1056/NEJMc2033369
20. Lee, M. H. *et al.* Neurovascular injury with complement activation and inflammation in COVID-19. Brain **145**, 2555–2568 (2022). https://doi.org:10.1093/brain/awac151
21. Constant, O. *et al.* SARS-CoV-2 Poorly Replicates in Cells of the Human Blood-Brain Barrier Without Associated Deleterious Effects. Front Immunol **12**, 697329–697329 (2021). https://doi.org:10.3389/fimmu.2021.697329
22. DeOre, B. J., Tran, K. A., Andrews, A. M., Ramirez, S. H. & Galie, P. A. SARS-CoV-2 Spike Protein Disrupts Blood-Brain Barrier Integrity via RhoA Activation. J Neuroimmune Pharmacol **16**, 722–728 (2021). https://doi.org:10.1007/s11481-021-10029-0
23. Kim, E. S. *et al.* Spike Proteins of SARS-CoV-2 Induce Pathological Changes in Molecular Delivery and Metabolic Function in the Brain Endothelial Cells. Viruses **13**, 2021 (2021). https://doi.org:10.3390/v13102021
24. Savarraj, J. *et al.* Brain injury, endothelial injury and inflammatory markers are elevated and express sex-specific alterations after COVID-19. J Neuroinflammation **18**, 277–277 (2021). https://doi.org:10.1186/s12974-021-02323-8
25. Wenzel, J. *et al.* The SARS-CoV-2 main protease M(pro) causes microvascular brain pathology by cleaving NEMO in brain endothelial cells. Nat Neurosci **24**, 1522–1533 (2021). https://doi.org:10.1038/s41593-021-00926-1
26. Zhang, L. *et al.* SARS-CoV-2 crosses the blood-brain barrier accompanied with basement membrane disruption without tight junctions alteration. Signal Transduct Target Ther **6**, 337–337 (2021). https://doi.org:10.1038/s41392-021-00719-9

27. Zhou, Y. *et al.* Network medicine links SARS-CoV-2/COVID-19 infection to brain microvascular injury and neuroinflammation in dementia-like cognitive impairment. Alzheimers Res Ther **13**, 110–110 (2021). https://doi.org:10.1186/s13195-021-00850-3
28. Bocci, M. *et al.* Infection of Brain Pericytes Underlying Neuropathology of COVID-19 Patients. Int J Mol Sci **22**, 11622 (2021). https://doi.org:10.3390/ijms222111622
29. Fitsiori, A., Pugin, D., Thieffry, C., Lalive, P. & Vargas, M. I. COVID-19 is Associated with an Unusual Pattern of Brain Microbleeds in Critically Ill Patients. J Neuroimaging **30**, 593–597 (2020). https://doi.org:10.1111/jon.12755
30. Krasemann, S. *et al.* The blood-brain barrier is dysregulated in COVID-19 and serves as a CNS entry route for SARS-CoV-2. Stem Cell Reports **17**, 307–320 (2022). https://doi.org:10.1016/j.stemcr.2021.12.011
31. Pellegrini, L. *et al.* SARS-CoV-2 Infects the Brain Choroid Plexus and Disrupts the Blood-CSF Barrier in Human Brain Organoids. Cell Stem Cell **27**, 951–961.e955 (2020). https://doi.org:10.1016/j.stem.2020.10.001
32. Rhea, E. M. *et al.* The S1 protein of SARS-CoV-2 crosses the blood-brain barrier in mice. Nat Neurosci **24**, 368–378 (2021). https://doi.org:10.1038/s41593-020-00771-8
33. Schwabenland, M. *et al.* Deep spatial profiling of human COVID-19 brains reveals neuroinflammation with distinct microanatomical microglia-T-cell interactions. *Immunity* **54**, 1594–1610.e1511 (2021). https://doi.org:10.1016/j.immuni.2021.06.002
34. Yang, R. C. *et al.* SARS-CoV-2 productively infects human brain microvascular endothelial cells. J Neuroinflammation **19**, 149 (2022). https://doi.org:10.1186/s12974-022-02514-x
35. Buzhdygan, T. P. *et al.* The SARS-CoV-2 spike protein alters barrier function in 2D static and 3D microfluidic in-vitro models of the human blood-brain barrier. Neurobiology of disease **146**, 105131–105131 (2020). https://doi.org:10.1016/j.nbd.2020.105131
36. Montalvan, V., Lee, J., Bueso, T., De Toledo, J. & Rivas, K. Neurological manifestations of COVID-19 and other coronavirus infections: A systematic review. Clin Neurol Neurosurg **194**, 105921 (2020). https://doi.org:10.1016/j.clineuro.2020.105921
37. Ng Kee Kwong, K. C., Mehta, P. R., Shukla, G. & Mehta, A. R. COVID-19, SARS and MERS: A neurological perspective. J Clin Neurosci **77**, 13–16 (2020). https://doi.org:10.1016/j.jocn.2020.04.124
38. O'Doherty, L. *et al.* Study protocol for the St James's Hospital, Tallaght University Hospital, Trinity College Dublin Allied Researchers' (STTAR) Bioresource for COVID-19. HRB Open Res **5**, 20 (2022). https://doi.org:10.12688/hrbopenres.13498.1
39. Finlay, J. B. *et al.* Persistent post-COVID-19 smell loss is associated with inflammatory infiltration and altered olfactory epithelial gene expression. *bioRxiv*, 2022.2004.2017.488474 (2022). https://doi.org:10.1101/2022.04.17.488474
40. Zhou, G., Lane, G., Cooper, S. L., Kahnt, T. & Zelano, C. Characterizing functional pathways of the human olfactory system. eLife **8**, e47177 (2019). https://doi.org:10.7554/eLife.47177

41. Saive, A. L., Royet, J. P. & Plailly, J. A review on the neural bases of episodic odor memory: from laboratory-based to autobiographical approaches. Front Behav Neurosci **8**, 240 (2014). https://doi.org:10.3389/fnbeh.2014.00240
42. Douaud, G. *et al.* SARS-CoV-2 is associated with changes in brain structure in UK Biobank. Nature **604**, 697–707 (2022). https://doi.org:10.1038/s41586-022-04569-5
43. Sudre, C. H. *et al.* Attributes and predictors of long COVID. Nature Medicine **27**, 626–631 (2021). https://doi.org:10.1038/s41591-021-01292-y
44. Qin, Y. *et al.* Long-term microstructure and cerebral blood flow changes in patients recovered from COVID-19 without neurological manifestations. J Clin Invest **131** (2021). https://doi.org:10.1172/jci147329
45. Tian, T. *et al.* Long-term follow-up of dynamic brain changes in patients recovered from COVID-19 without neurological manifestations. JCI Insight **7** (2022). https://doi.org:10.1172/jci.insight.155827
46. Donegani, M. I. *et al.* Brain Metabolic Correlates of Persistent Olfactory Dysfunction after SARS-Cov2 Infection. Biomedicines **9** (2021). https://doi.org:10.3390/biomedicines9030287
47. Guedj, E. *et al.* (18)F-FDG brain PET hypometabolism in patients with long COVID. Eur J Nucl Med Mol Imaging **48**, 2823–2833 (2021). https://doi.org:10.1007/s00259-021-05215-4
48. Greene, C. *et al.* Microvascular stabilization via blood-brain barrier regulation prevents seizure activity. Nat Commun **13**, 2003 (2022). https://doi.org:10.1038/s41467-022-29657-y
49. Aleksovska, K. *et al.* Systematic Review and Meta-Analysis of Circulating S100B Blood Levels in Schizophrenia. PLOS ONE **9**, e106342 (2014). https://doi.org:10.1371/journal.pone.0106342
50. Thelin, E. P., Nelson, D. W. & Bellander, B.-M. A review of the clinical utility of serum S100B protein levels in the assessment of traumatic brain injury. Acta Neurochirurgica **159**, 209–225 (2017). https://doi.org:10.1007/s00701-016-3046-3
51. Abdelhak, A. *et al.* Blood GFAP as an emerging biomarker in brain and spinal cord disorders. Nature Reviews Neurology **18**, 158–172 (2022). https://doi.org:10.1038/s41582-021-00616-3
52. McCarthy, M. J. Circadian rhythm disruption in Myalgic Encephalomyelitis/Chronic Fatigue Syndrome: Implications for the post-acute sequelae of COVID-19. *Brain, Behavior*, & Immunity - Health **20**, 100412 (2022). https://doi.org:https://doi.org/10.1016/j.bbih.2022.100412
53. Montoya, J. G. *et al.* Cytokine signature associated with disease severity in chronic fatigue syndrome patients. Proc Natl Acad Sci U S A **114**, E7150-e7158 (2017). https://doi.org:10.1073/pnas.1710519114
54. Lee, W. K. *et al.* Exogenous Transforming Growth Factor-β in Brain-Induced Symptoms of Central Fatigue and Suppressed Dopamine Production in Mice. Int J Mol Sci **22** (2021). https://doi.org:10.3390/ijms22052580
55. Oh, J. *et al.* SARS-CoV-2 spike protein induces cognitive deficit and anxiety-like behavior in mouse via non-cell autonomous hippocampal neuronal death. Scientific Reports **12**, 5496 (2022). https://doi.org:10.1038/s41598-022-09410-7

56. Ryan, F. J. *et al.* Long-term perturbation of the peripheral immune system months after SARS-CoV-2 infection. BMC Medicine **20**, 26 (2022). https://doi.org:10.1186/s12916-021-02228-6
57. Phetsouphanh, C. *et al.* Immunological dysfunction persists for 8 months following initial mild-to-moderate SARS-CoV-2 infection. Nature Immunology **23**, 210–216 (2022). https://doi.org:10.1038/s41590-021-01113-x
58. Rass, V. *et al.* Neurological outcomes one year after COVID-19 diagnosis: a prospective longitudinal cohort study. Eur J Neurol (2022). https://doi.org:10.1111/ene.15307
59. Whitaker, M. *et al.* Persistent COVID-19 symptoms in a community study of 606,434 people in England. Nature Communications **13**, 1957 (2022). https://doi.org:10.1038/s41467-022-29521-z
60. Jackman, A. H. & Doty, R. L. Utility of a three-item smell identification test in detecting olfactory dysfunction. Laryngoscope **115**, 2209–2212 (2005). https://doi.org:10.1097/01.mlg.0000183194.17484.bb
61. Lechien, J. R. *et al.* Olfactory and gustatory dysfunctions as a clinical presentation of mild-to-moderate forms of the coronavirus disease (COVID-19): a multicenter European study. Eur Arch Otorhinolaryngol **277**, 2251–2261 (2020). https://doi.org:10.1007/s00405-020-05965-1
62. O'Keeffe, E. *et al.* Dynamic Blood-Brain Barrier Regulation in Mild Traumatic Brain Injury. Journal of neurotrauma **37**, 347–356 (2020). https://doi.org:10.1089/neu.2019.6483
63. Weissberg, I. *et al.* Imaging Blood-Brain Barrier Dysfunction in Football Players. JAMA Neurology **71**, 1453–1455 (2014). https://doi.org:10.1001/jamaneurol.2014.2682
64. Manjón, J. V. & Coupé, P. volBrain: An Online MRI Brain Volumetry System. Frontiers in Neuroinformatics **10** (2016). https://doi.org:10.3389/fninf.2016.00030

Tables 1-4

Tables 1-4 are available in the Supplementary Files section.

Figures

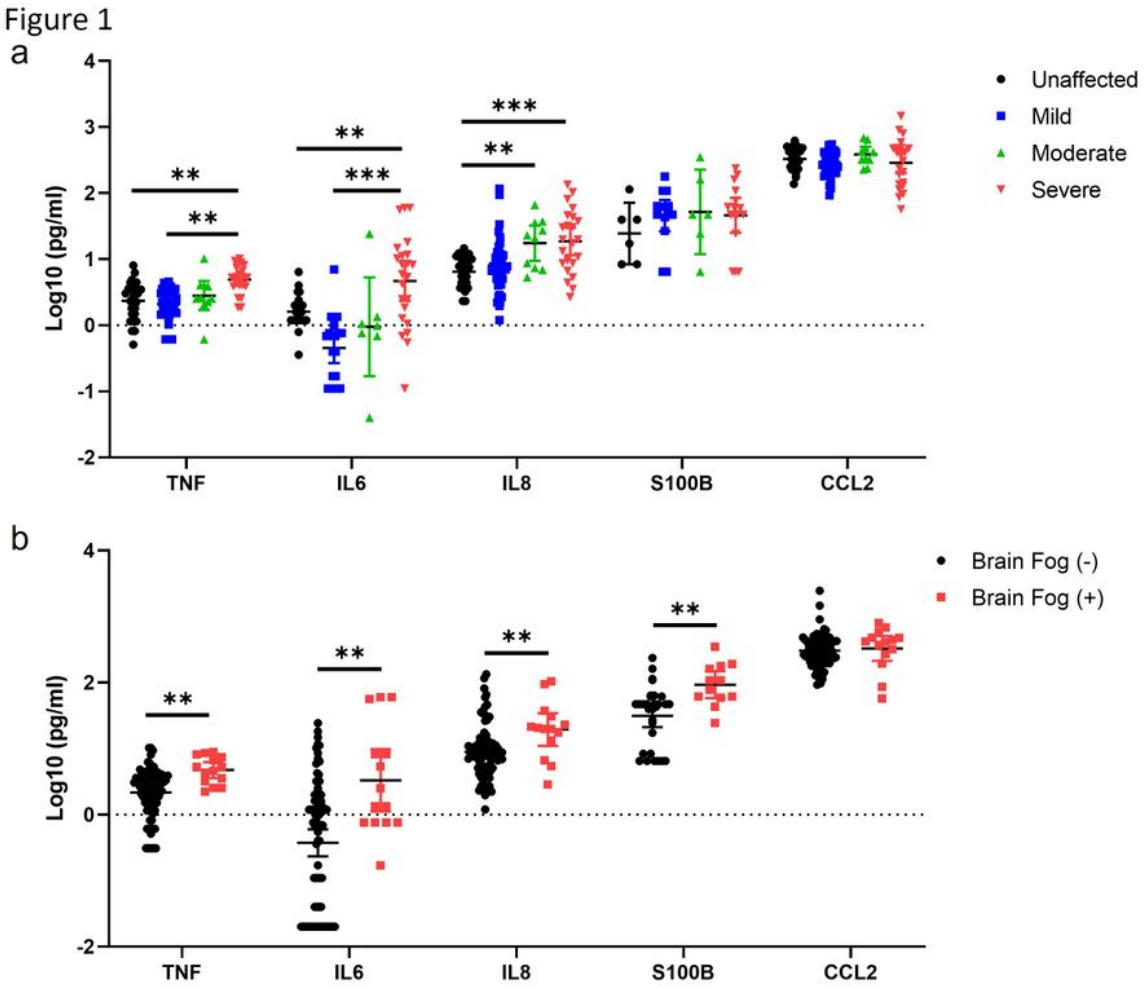

Figure 1

Inflammation and blood-brain barrier (BBB) permeability in acute COVID-19 infected cases. a) TNF, IL6, IL8, S100β and CCL2 serum concentrations in unaffected, mild, moderate, and severe SARS-CoV-2 infected patients. b) TNF, IL6, IL8, S100β and CCL2 serum concentrations in neurological SARS-CoV-2 infected patients. Data represent means with 95% confidence intervals; each datapoint represents one

patient. Data analysed by MANCOVA with age, sex and WHO severity as covariates. *p<0.05; **p<0.01; ***p<0.001.

Figure 2

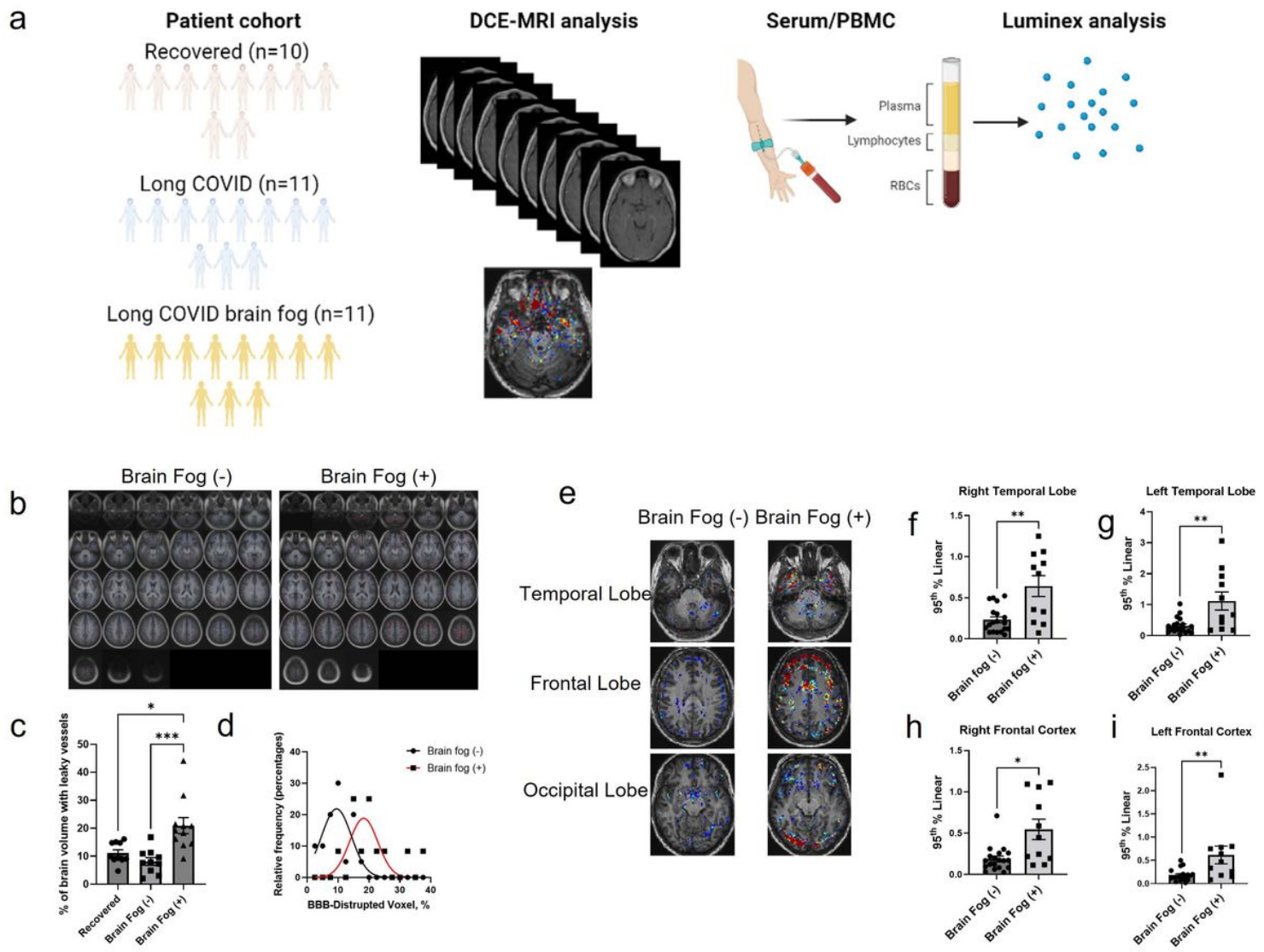

Figure 2

BBB disruption in Long COVID-associated cognitive impairment. a) Patient cohort for dynamic contrast-enhanced magnetic resonance imaging (DCE-MRI). b) Averaged BBB permeability maps in non-brain fog and brain fog cases. c) There were significantly increased percentage of brain volume with leaky blood vessels in the brain fog cohort compared to recovered and non-brain fog cases. d) Frequency distribution of the percentage of BBB disrupted voxels in the non-brain fog and brain fog cases. e) Representative BBB permeability maps at the level of the temporal lobe, frontal lobe and occipital lobe showing enhanced BBB permeability in brain fog cases. f-i) Quantification of regional BBB permeability in the right and left temporal lobe and right and left frontal cortex. Data represent means ± s.e.m.; each datapoint represents one patient. Data analysed by ANCOVA with age and sex as covariates. *p<0.05; **p<0.01; ***p<0.001.

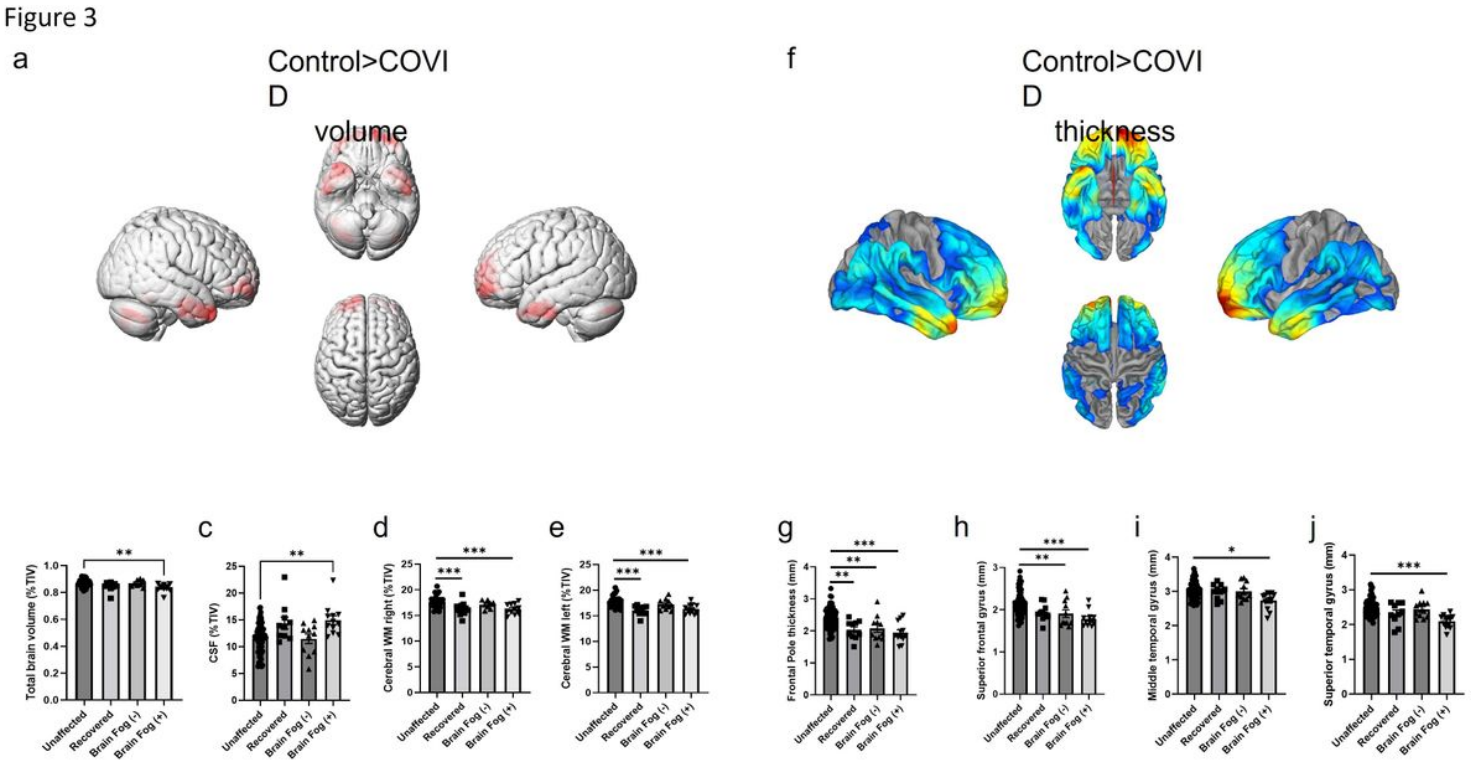

Figure 3

COVID-associated brain changes. a) Voxel-based morphometry map indicating brain regions with reduced volume in patients with prior SARS-CoV-2 infection. b-e) Group-wise comparison of brain volume in unaffected, recovered, long COVID and brain fog groups. f) Surface-based morphometry map indicating brain regions with reduced cortical thickness in patients with prior SARS-CoV-2 infection. g-j) Group-wise comparison of cortical thinning in unaffected, recovered, long COVID and brain fog groups. Maps generated with CAT12 toolbox in SPM12 running on MATLAB 2021a. Groups compared with unpaired t-test with family-wise error <0.05, adjusted for age, sex and TIV. Volumetric and thickness region of interest measurements were obtained from VolBrain. Groups were compared with ANCOVA adjusted for age and sex. Data represents means ± s.e.m.; each datapoint represents one patient. *p<0.05, **p<0.01, ***p<0.001.

Figure 4

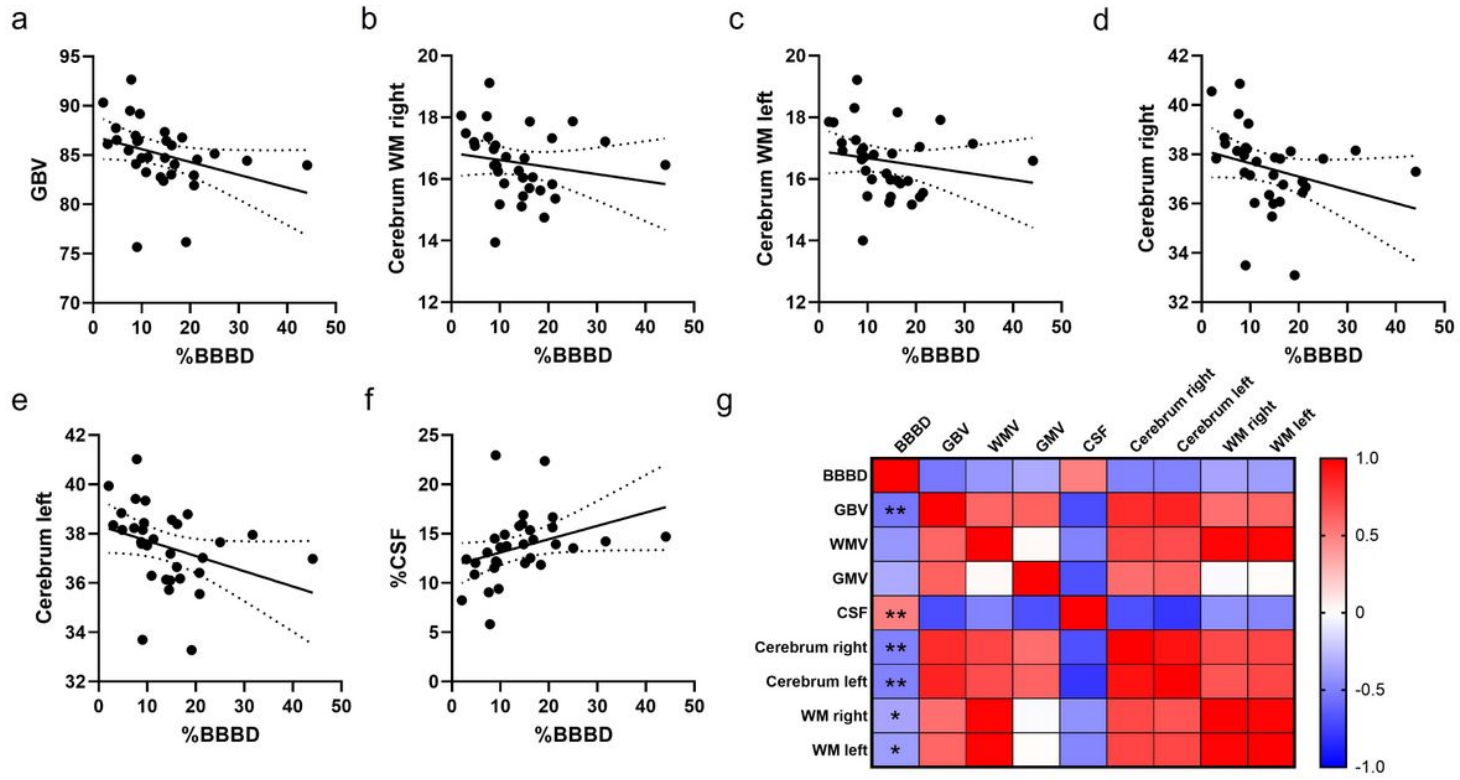

Figure 4

BBB permeability is associated with structural brain changes. a-f) Spearman partial correlation between the percentage of BBB disrupted voxels and white matter volume and global brain volume. g) Heat-map of Spearman correlations between BBB permeability and global brain volume. Each datapoint represents one patient. Spearman partial correlation analysis for all panels adjusted for age, sex and TIV. *p<0.05; **p<0.01.

Figure 5

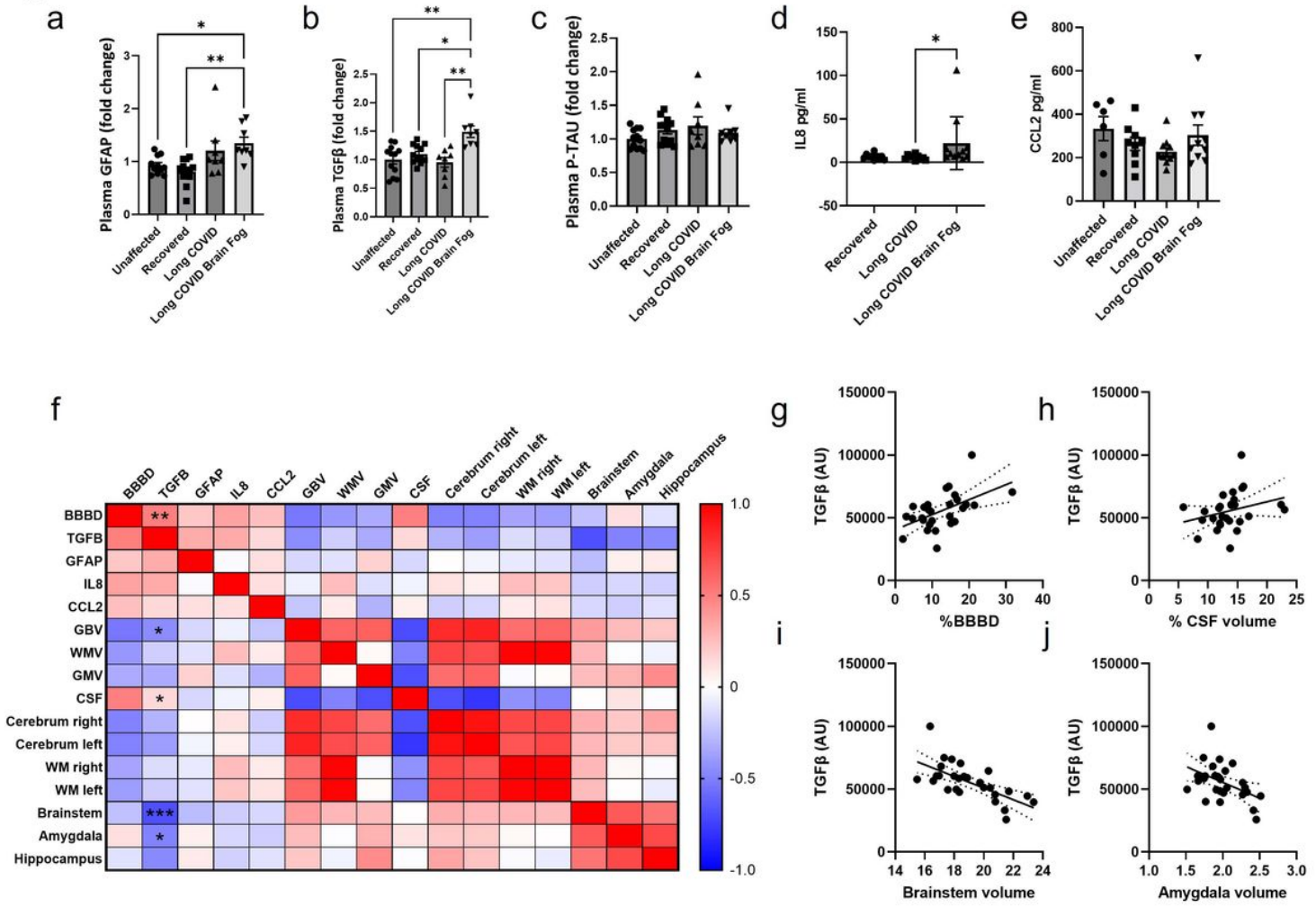

Figure 5

Plasma TGFβ is associated with increased BBB permeability. a-e) Serum and plasma analysis of GFAP, TGFβ, P-TAU, IL8 and CCL2 in recovered, non-brain fog and brain fog cohort. f) Spearman partial correlations between analyte levels and BBB permeability and global brain volume measurements. g-i) Spearman correlation between levels of TGFβ and percentage BBB disruption, percentage CSF volume, brainstem volume and amygdala volume. Data represent means ± s.e.m.; each datapoint represents one patient. Kruskal Wallis test for a-e, Spearman partial correlation analysis controlling for age, sex and TIV for f-j. *p<0.05; **p<0.01.

Figure 6

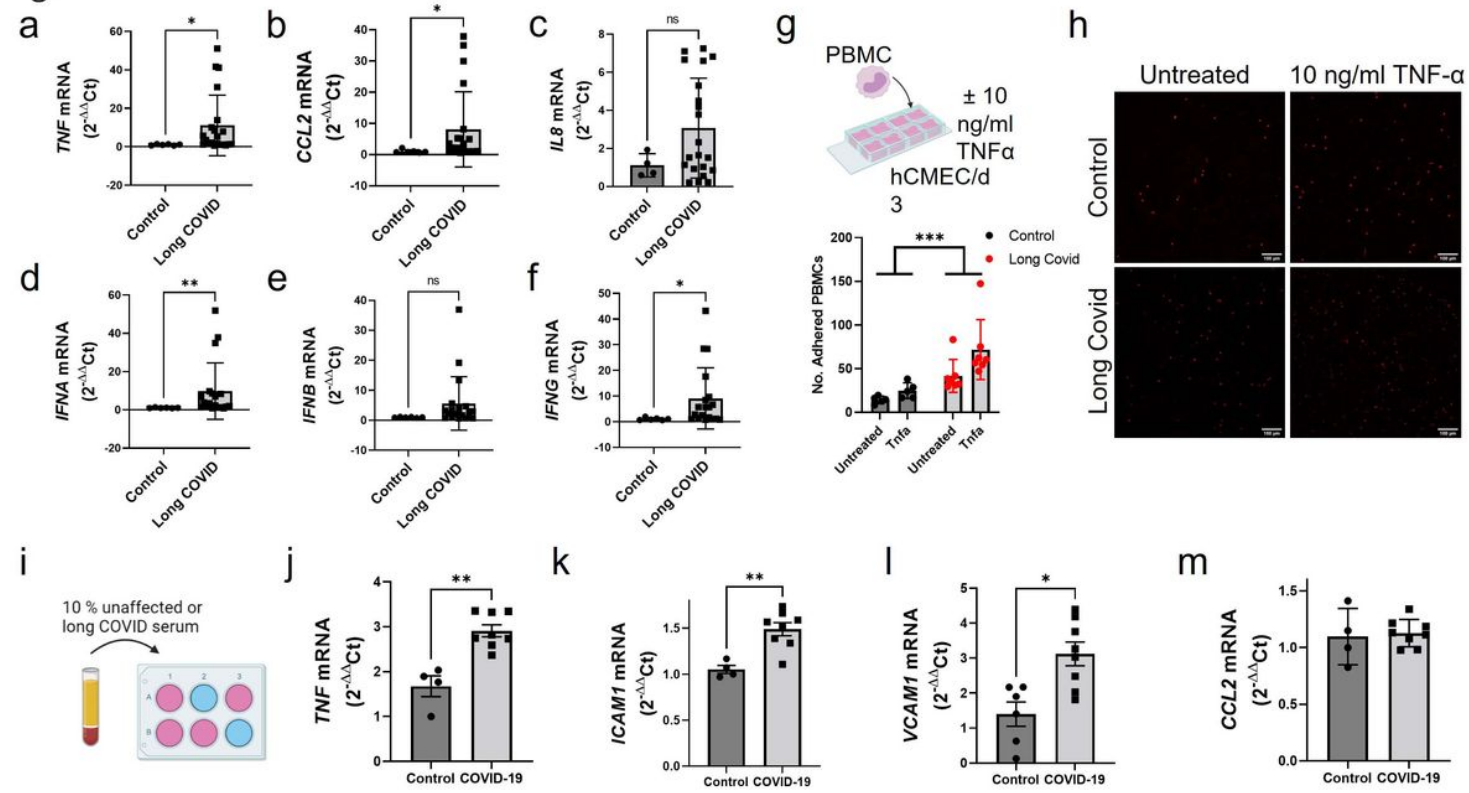

Figure 6

Immunovascular dysfunction in long COVID blood samples. a-f) Gene expression changes in unaffected and long COVID PBMCs. g-h) PBMC adhesion assay on human brain endothelial cells (hCMEC/d3) in the presence or absence of 10 ng/ml TNF. i-l) Gene expression changes in hCMEC/d3 cells exposed to control or long COVID serum. Data represent means ± s.e.m.; each datapoint represents one patient. Unpaired t-test for gene expression data, two-way ANOVA for adhesion assay. *p<0.05; **p<0.01; ***p<0.001.

Supplementary Files

This is a list of supplementary files associated with this preprint. Click to download.

- Tables.pdf
- SupplementaryFigures.pdf